An Adaptive Beamformer Based on Adaptive Covariance Estimator

Lay Teen Ong[*]

Abstract—Based on the Minimum Variance Distortionless Response-Sample Matrix Inversion (MVDR-SMI) method, we propose a novel Adaptive Covariance Estimator (MVDR-ACE) beamformer for adaptation to multiple interference environments. The MVDR-ACE beamformer iteratively determines a minimum number of data samples required while maintaining its average signal-to-interference-noise to be within 3 dB from the performance of a theoretical optimum MVDR beamformer and meeting an instantaneous interference cancellation requirement. Finally, based on numerical simulations, we analyze and validate the performance of the MVDR-ACE beamformer. We also compare its performance to the conventional MVDR-SMI beamformer that uses a fixed data sample in its covariance estimator.

1. INTRODUCTION

Adaptive beamforming techniques have been widely used in adaptive array systems for radar, audio, sonar, satellite and wireless communications applications. The Minimum Variance Distortionless Response (MVDR) beamformimg is a classical technique used to achieve maximum signal-to-interference-noise (SINR) in an adaptive array system [1, 2]. However, traditional MVDR beamforming technique is known to experience performance degradation and increased computation complexity when used in practical environments. For instance, any mismatch in sensor array responses, mutual coupling of the array or imperfect array calibration would result in the beamformer to wrongly cancel the desire signal due to look directions error. Many approaches have been proposed to improve the robustness of the beamformer [3–8]. For example, the diagonal loading technique [3, 4] has been a widespread approach to provide robustness but the choice of an optimum diagonal loading factor is not clear in practice and is still being researched on [5]. Alternatively, variants of linearly constrained minimum variance type beamformers researched on for beamforming robustness include work in [6, 7], where addition linear constraints are imposed to broaden the main beam of the beampattern. In [8], robust beamforming based on the multi-parametric quadratic programming for nulling level control was proposed to control the interference angle spread areas within a prescribed threshold. On the other hand, in applications where planar array of higher number of antenna elements are used, the use of adaptive Genetic Algorithms for adaptively control the antenna elements had shown advantages in terms of performance and computational complexity [9, 10].

To obtain the optimum weights of the array, an ideal MVDR beamformer requires an exact covariance matrix of the data signal arriving at the array. In this case, apriori knowledge of the signal environment of the MVDR beamformer is necessary. Subsequently, a best set of antenna weights is computed based on the covariance matrix of the signal. In practice, it is not feasible to calculate the exact covariance matrix so an estimate of the covariance matrix is used. In addition, as the signal environment changes, the weight vectors must be updated or adapted to reflect the varying conditions. This adaptive computation of covariance estimates results in a significant increase in the computational load of the array processor. Therefore, the number of data samples used for the covariance matrix estimate is usually small to ensure that the computational load is plausible. However, this results in some

* Corresponding author: Lay Teen Ong (tslolt@nus.edu.sg).
The author is with the Temasek Laboratories, National University of Singapore, Singapore 117411, Singapore.

degradation in performance and the severity of degradation is dependent on whether the desired signal is present or absent in the sampled data. When the desired signal is present, inaccurate estimations from the limited data samples result in cancelling of the desired signal, resulting in sub-optimal SINR and a signal with underestimated power [11]. In [12, 13], analytical and Monte-Carlo simulation results showed that a higher number of data samples is required to approach SINR convergence when the desired signal is present in the covariance matrix. On the other hand, when the desired signal is absent or when interference signals dominate, interference suppression is one figure of merit to focus. [11, 14] have shown that relatively fewer samples are needed for effective interference suppression, but the adaptive algorithm generates a distorted array pattern with high sidelobe levels at angles where the interferences are not present. This distorted pattern affects systems which are vulnerable to clutter signals in the sidelobes and mainlobe.

In this work, we focus on the effect of data sample size on the interference cancellation capability and the SINR of the MVDR beamformers. In particular, our interest is to perform beamforming and at the pre-correlation stage of a spread spectrum system over multiple numbers of interferences. We also consider an N-element circular array antenna before the beamformer. One specific application of this beamformer design is as an interference cancellation appliqué in Global Navigation Satellite System (GNSS) receivers. As the desired signal received is very weak when it arrives at the front-end of the spread spectrum receiver, the system is very susceptible to interferences. Therefore, we study the performance of the MVDR beamformers in an interference-dominance environment, and specifically, when multiple uncorrelated interferences are present. In the second part of this work, we propose a simple but novel algorithm that uses an Adaptive Covariance Estimator (ACE) to iteratively achieve a sufficiently small data samples for adequate interference cancellation. In precise, the proposed MVDR-ACE beamformer iteratively determines a minimum number of data samples to meet its instantaneous interference cancellation requirement while maintaining its average SINR to be within a 3 dB ratio of a theoretical MVDR beamformer. In comparison, several earlier works have researched on deriving, on average, a fixed number of samples to achieve an average output SINR using Sample Matrix Inversion (SMI) estimator [13, 15–17]. In [18], an iterative algorithm for MVDR filter through auxiliary vector had been designed that generates a sequence of filter estimation over a finite sample size. However, to the best of the author's knowledge, no work has been published on algorithm to adjust the sample size in accordance to variation in the interference environment.

The SMI approach has several advantages. It is well known for its speed advantage and is also noted to be most value in complicated interference environments where the number of interference sources is large. However, it is only appropriate for stationary environment and not for interference parameters variation [19]. These imply a particular sample size determined for one channel condition may not be appropriate for another channel condition. In the work, we employ a SMI based MVDR beamformer for operation in complex interference environments. To address the variation of the interference or channel conditions, we propose to adapt the SMI data samples in accordance to channel condition but remains sufficient to maintain the required SINR performance of the beamformer. Finally, we use Monte-Carlo simulations to validate the performance of our proposed algorithm and make comparisons to the conventional MVDR-SMI that uses fixed data sample.

The remainder of this paper is organized as follows. In Section 2 we describe the system model of an adaptive array system and the conventional MVDR beamformer. We propose an adaptive algorithm using an Adaptive Covariance Estimator in Section 3. In Section 4, we evaluate the performance of the conventional MVDR beamformer and validate the performance of our proposed MVDR-ACE beamformer using numerical simulations. Finally, conclusions are drawn in Section 5.

2. THEORETICAL MODELS

2.1. Signal Model

Figure 1 shows the generic block diagram of an adaptive N-element array. We consider a uniform N-element circular array with a radius r from the center of the circle shown in Figure 2. The N element array receives one desired signal and $M - 1$ number of interference signals. The array observations vector $\mathbf{x}(t)$ at time t can be written as

$$\mathbf{x}(t) = \mathbf{A}(\theta, \phi)\, \mathbf{s}(t) + \mathbf{n}(t), \tag{1}$$
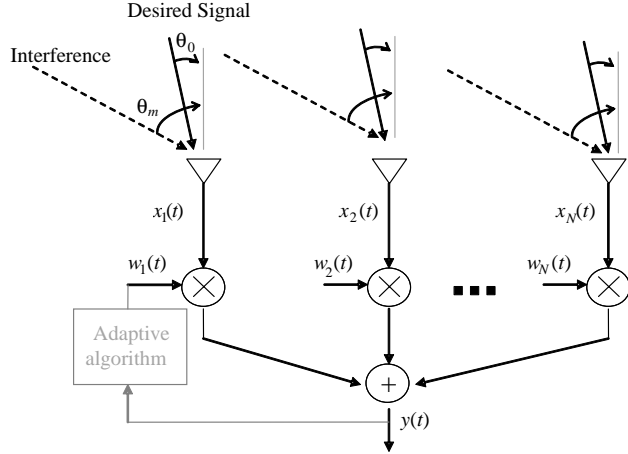
Figure 1. Block diagram of an N-element adaptive array.
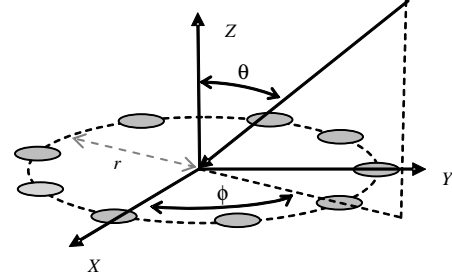
Figure 2. Geometry structure of a uniform N-element circular array.

where $\mathbf{s}(t) = [s_0(t), s_1(t), \ldots, s_{M-1}(t)]^T$ is an $M \times 1$ signal vector whose row components are the uncorrelated desired and interference signal sources and T denotes matrix transpose.

$\mathbf{A}(\theta, \phi) = [\mathbf{a}(\theta_0, \phi_0), \mathbf{a}(\theta_1, \phi_1), \ldots, \mathbf{a}(\theta_{M-1}, \phi_{M-1})]$ is an $N \times M$ matrix whose columns. $\mathbf{a}(\theta_i, \phi_i) = [1, e^{j\beta r \sin(\theta_i) \cos(\phi_i - \phi_1)}, e^{j\beta r \sin(\theta_i) \cos(\phi_i - \phi_2)}, \ldots, e^{j\beta r \sin(\theta_i) \cos(\phi_i - \phi_{N-1})}]^T$ are steering vectors of the antenna array, where $i = 0, \ldots, M-1$, θ_i and ϕ_i are the respective azimuth and elevation angle of the signal $s_i(t)$. $\beta = 2\pi/\lambda$ defines the wave number where λ is the wavelength of the signal. $\mathbf{n}(t)$ is an $N \times 1$ noise vector whose row components are independent additive white Gaussian noise with zero mean and variance σ_n^2. The output of the beamformer is

$$y(t) = \mathbf{w}(t)^H \mathbf{x}(t), \tag{2}$$

where $\mathbf{w}(t) = [w_1(t), w_2(t), \ldots, w_N(t)]^T$ is a $1 \times N$ weight vector whose components correspond to the weights of the beamformer, and H denotes Hermitian transpose. The exact covariance matrix of the total received signal is $\mathbf{R} = E(\mathbf{x}(t)\mathbf{x}^H(t))$, where $E(\cdot)$ denotes the expectation operator. When the desired signal and the interference signals are uncorrelated with each other, $\mathbf{x}(t) = \mathbf{x}_D(t) + \mathbf{x}_I(t) + \mathbf{n}(t)$ where $\mathbf{x}_D(t) = \mathbf{a}(\theta_0, \phi_0)s_0(t)$ and $\mathbf{x}_I(t) = \sum_{i=1:M-1} \mathbf{a}(\theta_i, \phi_i)s_i(t)$ are the desired and interference signals respectively. Note that $\mathbf{R} = \mathbf{R}_D + \mathbf{R}_I + \mathbf{R}_n$ where $\mathbf{R}_D = E(\mathbf{x}_D(t)\mathbf{x}_D^H(t))$ is the desired signal covariance matrix, $\mathbf{R}_I = E(\mathbf{x}_I(t)\mathbf{x}_I^H(t))$ and $\mathbf{R}_n = \sigma_n^2\mathbf{I}$ are the total interference and white noise covariance matrix respectively. σ_n^2 and $\mathbf{I}$ denote the noise power and identity matrix. Here, we assume that the received signal is significantly below the noise floor of the receiver so the $\mathbf{R}_D$ term can be ignored and the covariance matrix of the system is reduced to $\mathbf{R} = \mathbf{R}_I + \mathbf{R}_n$.

2.2. Theoretical MVDR Beamformer

MVDR beamforming is a classical method that minimizes the array output power subject to a constraint of unity gain in the look direction of the array [1, 2]. Mathematically, this is expressed as

$$\min_{\mathbf{w}} \mathbf{w}^H \mathbf{R} \mathbf{w} \quad \text{s.t. } \mathbf{w}^H \mathbf{a}(\theta_0, \phi_0) = 1, \tag{3}$$

where $\mathbf{a}(\theta_0, \phi_0)$ is the steering vector of the desired signal. The solution to the optimization problem can be shown to be

$$\mathbf{w} = \frac{\mathbf{R}^{-1}\mathbf{a}(\theta_0, \phi_0)}{\mathbf{a}(\theta_0, \phi_0)^H \mathbf{R}^{-1}\mathbf{a}(\theta_0, \phi_0)}. \tag{4}$$

In general, the figure of merit of the beamformer can be obtained from its SINR and cancellation capability. The SINR parameter at the output of the array can be computed as

$$\text{SINR} = \mathbf{w}^H \mathbf{R}_D \mathbf{w} / \mathbf{w}^H \mathbf{R} \mathbf{w}. \tag{5}$$

Alternatively, the improvement factor (IF) of the beamformer can be represented via the SINR parameter, and is expressed as, IF $= \frac{\text{SINR}}{\text{SINR}_{\text{IN}}}$, which defines the ratio of the SINR at the output of the array (SINR) to the SINR measured at the input of an element of the array (SINR$_{\text{IN}}$).

The cancellation capability of the beamformer can be determined through either the cancellation ratio (CR), null-depth or array pattern of the beamformer. Commonly, CR is expressed as [20, 21],

$$CR = \frac{P_{non\_adpt}}{P_{adpt}} \tag{6}$$

which defines the ratio of the output power of the non-adaptive (or quiescent state) array (P_{non_adpt}) to the output power of the adapted array (P_{adpt}). Alternatively, the interference cancellation capability can be derived from the array pattern, and is measured by considering a unit amplitude test signal propagating into the antenna array from angle (θ_t, ϕ_t) and measuring the array output signal power [22]. From the adapted pattern, the null-depth of the interferences can be determined from the depth of the null placed at the interference location with respect to the peak of the pattern [21].

2.3. Sample Matrix Inversion for MVDR Beamformer

Sample Matrix Inversion (SMI) [15, 23] is a fast adaptive beamforming/nulling technique because it directly calculates the covariance matrix, thereby avoiding the problem of eigenvalue spread, which often limits the convergence rate for close-loop algorithms (such as the least mean square algorithm [24]). SMI is based on the maximum likelihood estimate of the data covariance matrix and the numerical inversion of the matrix to find optimum weight values. An estimate of the covariance matrix, $\hat{\mathbf{R}}$, can be derived from [15],

$$\hat{\mathbf{R}} = 1/K \sum_{k=1}^{K} \mathbf{x}(k) \mathbf{x}(k)^{H}, \tag{7}$$

where K is the number of snapshots observed every time instance t. Therefore, the weight vector at t becomes

$$\hat{\mathbf{w}} = \frac{\hat{\mathbf{R}}^{-1} \mathbf{a}(\theta_0, \phi_0)}{\mathbf{a}(\theta_0, \phi_0)^{H} \hat{\mathbf{R}}^{-1} \mathbf{a}(\theta_0, \phi_0)}. \tag{8}$$

Reed et al. [15] have shown that in order to achieve an average loss ratio of less than 3 dB in the output SINR, $K \geq 2N - 3$ samples of data are required. The threshold is obtained by comparing expected loss in power to the optimum case and expressed as,

$$E\left(\rho\left(\hat{\mathbf{R}}\right)\right) = (K + 2 - N)/(K + 1), \tag{9}$$

where $\rho(\cdot)$ is a random variable [15]. As this is a random variable, there is a probability that the loss ratio will be more than or less than 3 dB from optimum. In practice, an exact number of snapshots data is required. This can be determined using a computer simulation [15], where a range of snapshots $K \geq 2N - 3$ are used to compute the respective SINR values of the beamformer assuming a signal environment. In general, as K gets large, $\hat{\mathbf{R}}$ approaches the optimum covariance matrix $\mathbf{R}$. This means that in a practical system, to derive an exact snapshot size, K has to be pre-determined through a calibration process, and an apriori interference/channel condition has to be assumed in the calibration process. Depending on the environments and applications, K would have to be updated as channel condition varies. Therefore, an adaptive algorithm or a re-calibration process is required. In this work, we propose an adaptive approach to determine K as the interference environment changes. In our proposed algorithm, we aim to maintain smaller number of snapshots as channel condition changes but remains sufficient to maintain the required SINR performance of the beamformer.

3. ADAPTIVE BEAMFORMER BASED ON ADAPTIVE COVARIANCE ESTIMATOR AND INTERFERENCE CANCELLATION

We propose an adaptive covariance estimator whose sample size is variable in accordance to certain conditions. That is,

$$\tilde{\mathbf{R}}\left(t\right) = 1/L\left(t\right) \sum_{l=1}^{L(t)} \mathbf{x}\left(l\right) \mathbf{x}^{H}\left(l\right), \tag{10}$$

where $L(t)$ denotes the sample size that is adaptive in time instance t. This is in contrast to the conventional MVDR-SMI estimator (7) where the sample size is fixed at K. The corresponding adaptive weight vector becomes

$$\tilde{\mathbf{w}}\left(t\right) = \frac{\tilde{\mathbf{R}}\left(t\right)^{-1} \mathbf{a}\left(\theta_0, \phi_0\right)}{\mathbf{a}\left(\theta_0, \phi_0\right)^{H} \tilde{\mathbf{R}}\left(t\right)^{-1} \mathbf{a}\left(\theta_0, \phi_0\right)}. \tag{11}$$

Note that t is included explicitly in the estimates (10) and (11) as they are obtained iteratively in time instances. For example, in a block fading channel model, t will correspond to the time-state over a block of sample size $L(t)$. In the proposed algorithm, $L(t)$ is adjusted in accordance to the following conditions,

$$L\left(t+1\right) = \begin{cases} L_0, & t = 0, \\ L\left(t\right) + \Delta l, & \left(\gamma\left(t\right) < CRT\right) \text{ and } \left(L\left(t\right) < L_{\max}\right), \\ L\left(t\right) - \Delta l, & \left(\gamma\left(t\right) \geq CRT\right) \text{ and } \left(L\left(t\right) > L_{\min}\right), \\ L\left(t\right), & \text{otherwise.} \end{cases} \tag{12}$$

The time instances t and $t-1$ denote, respectively, the current and previous time-state of the estimation. Δl is the step-size change in the number of snapshot. The first condition in (12) initializes the iterative loop at $t = 0$. For an invertible $\tilde{\mathbf{R}}(\cdot)$, L_0 is set a minimum value of $2N$. The second and third condition vary the adaptive snapshot size $L(t+1)$ in accordance to an instantaneous cancellation ratio, $\gamma(t)$, meeting a pre-determined cancellation ratio target (CRT). $\gamma(t)$ defines a figure of merit for the instantaneous interference cancellation capability of the beamformer and is expressed in (13). The choice of the CRT value will depend on the system requirement on interference cancellation. When an N-element array is used, the CRT is bounded by a theoretical limit of INR $+10 \times \log 10(N)$ [20], where INR denotes the interference to noise ratio at the input of an element of the array. The second and third conditions also subject $L(t+1)$ to a maximum and minimum snapshot size constraints, $L_{\max}$ and $L_{\min}$ respectively. We set $L_{\max}$ to a sufficient large value so that the beamformer is on average maintaining the 3 dB ranges of its optimum performance (see Section 2.3), and set $L_{\min}$ to minimum of $2N$ for an invertible $\tilde{\mathbf{R}}(\cdot)$. In other conditions, $L(t+1)$ remains unchanged.

As we consider that the desired signal is significantly below the noise floor level and that interference signals are dominant, the ratio of the power measured at the output of the non-adapted and adapted array, as expressed in (6), will form the interference cancellation ratio of the beamformer. Therefore, we can compute $\gamma(t)$ as

$$\gamma\left(t\right) = \frac{P_{non\_adapt}}{P_{adapt}} = \frac{\tilde{\mathbf{w}}_Q^{H} \tilde{\mathbf{R}}\left(t\right) \tilde{\mathbf{w}}_Q}{\tilde{\mathbf{w}}\left(t\right)^{H} \tilde{\mathbf{R}}\left(t\right) \tilde{\mathbf{w}}\left(t\right)}, \tag{13}$$

where $\tilde{\mathbf{R}}(t)$ and $\tilde{\mathbf{w}}(t)$ are iterative values obtained from (10) and (11) respectively. $\mathbf{w}_Q$ is the weight vector of the quiescent state of the array and can be computed initially during the calibration process.

In summary, we have proposed an adaptive covariance estimator with two primary characteristics. First, a snapshot size that comprises of small number of data samples is adjusted iteratively. This snapshot is sufficient for the beamformer to meet its interference cancellation ratio requirement while maintaining its average SINR performance to be within a 3 dB performance of an optimum beamformer. Second, a larger snapshot size will be set if, on average, the beamformer could not achieve its cancellation ratio requirement. We expect this to happen when the beamformer exhausts it degree-of-freedoms when dealing with a high number of interference signals.

4. SIMULATIONS AND RESULTS ANALYSIS

We used Monte-Carlo simulations to verify the performance of the MVDR-SMI beamformers. An 8-element circular array with radius half wavelength was used. We consider an 8-element array because it is a realistic size in terms of compactness and interference mitigation performance when used for GNSS applications [25, 26]. The desired signal was assumed to arrive from the broadside direction $(0°, 0°)$ and the signal power is 20 dB below the noise level. The interference environment considered consists of one to seven uncorrelated signals with different Angle-of-Arrivals (AOAs), all having the same interference-to-noise power ratio (INR) of 40 dB. The two interference scenarios considered are summarized in Table 1 and Table 2. Scenario A emulates a situation where the interference signals arrive only from the XZ plane of the top hemispherical (Figure 2) while scenario B is for the situation where the interference signals arrive at arbitrary angles of the top hemispherical plane. We generated a sequence of the desired and interference signal data, each consisting of M zero-mean complex Gaussian random variables whose variance is its signal powers. We generated $\mathbf{n}(t)$ consisting of N zero-mean, unit variance and independent complex Gaussian random variables. The simulation was repeated for $T = 3000$ trials and each trial (every t instance) consists of K snapshot of signals data. The instantaneous parameters (e.g., $L(t)$, $\mathrm{ICR}_m(t)$) were computed at every t instance while their respective average parameters (e.g., SINR, IF) were computed as an ensemble average over the T trials.

Table 1. Interference setting for scenario A.

# of interference signals	(Elevation, Azimuth): (θ, ϕ)
1	$(80°, 0°)$
2	$(80°, 0°)$, $(60°, 180°)$
3	$(80°, 0°)$, $(70°, 0°)$, $(60°, 180°)$
4	$(80°, 0°)$, $(70°, 0°)$, $(60°, 180°)$, $(85°, 180°)$
5	$(80°, 0°)$, $(70°, 0°)$, $(60°, 180°)$, $(75°, 180°)$, $(85°,180°)$
6	$(80°, 0°)$, $(70°, 0°)$, $(50°, 180°)$, $(60°, 180°)$, $(75°,180°)$, $(85°,18 0°)$
7	$(80°, 0°)$, $(70°, 0°)$, $(60°, 0°)$, $(50°, 180°)$, $(60°, 180°)$, $(75°, 180°)$, $(85°, 180°)$

Table 2. Interference setting for scenario B.

| # of interference signals	(Elevation, Azimuth): (θ, ϕ)
1	$(80°, 0°)$
2	$(80°, 0°)$, $(70°, 60°)$
3	$(80°, 0°)$, $(70°, 60°)$, $(50°, 300°)$
4	$(80°, 0°)$, $(70°, 60°)$, $(50°, 300°)$, $(60°, 0°)$
5	$(80°, 0°)$, $(70°, 60°)$, $(50°, 300°)$, $(60°, 0°)$, $(55°, 60°)$
6	$(80°, 0°)$, $(70°, 60°)$, $(50°, 300°)$, $(60°, 0°)$, $(55°, 60°)$,$(85°, 120°)$
7	$(80°, 0°)$, $(70°, 60°)$, $(50°, 300°)$, $(60°, 0°)$, $(55°, 60°)$, $(85°, 120°)$, $(65°, 210°)$

4.1. MVDR-SMI Beamformer of Finite Sample-size

First, we analyse the results of a conventional MVDR-SMI beamformer employed with a finite snapshot size. We use $K = [10, 20, 30, 40, 50, 100, 150, 200, 400, 3000]$ for all the interference cases of scenario A and B. We are interested in determining the snapshot size that results in the beamformer when, i) approaching its IF (correspondingly the SINR) convergence and ii) achieving within the 3 dB of this converged value.

Figure 3 and Figure 4 show the average IF values for scenarios A and B, respectively. The results show that the beamformer converges at $K = 3000$ for all interference cases. However, it is interesting to note that at scenario A cases with 6 or 7 interference signal, the IF of the beamformer decreases slightly (within 1 dB) as K increases. This reflects the random phenomena of the average SINR values against the snapshots as expressed in (9), and that the IF ratio can be more than or less than 3 dB from optimum. In scenario A (Figure 3), $K = 20$ is the minimum snapshot value required by the beamformer to achieve a result that is within 3 dB of converged performance for all the interference cases. However, in scenario B (Figure 4), a beamformer with $K = 20$ snapshots can maintain the IF to within a 3 dB range for only a maximum of 3 interferences. To stay within the 3 dB range at all the interference cases, the beamformer requires $K = 200$ snapshots.
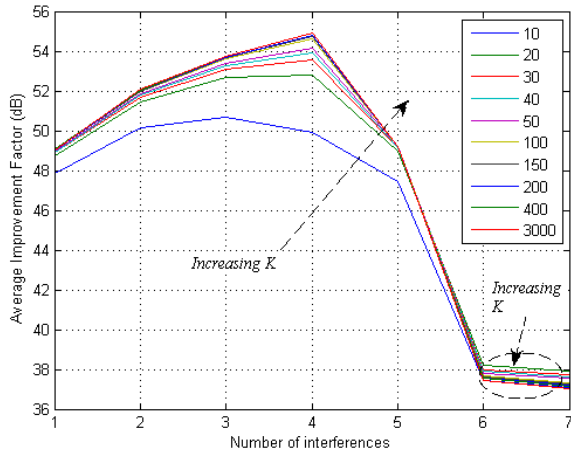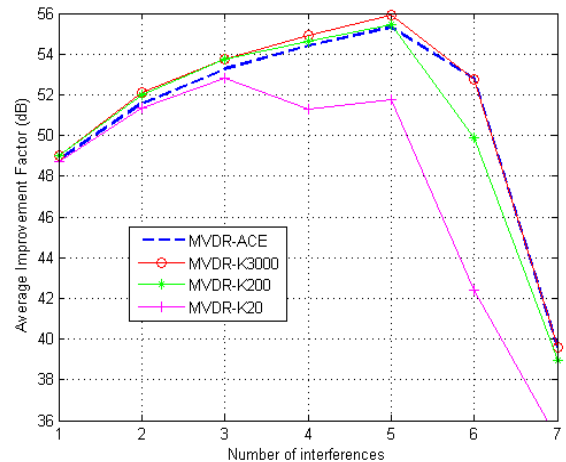
Figure 3. Scenario A: average improvement factor versus the number of interferences for MVDR-SMI at various snapshot sizes, K.
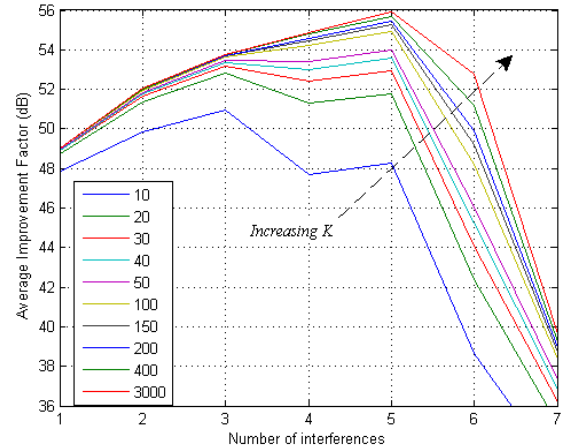
Figure 4. Scenario B: average improvement factor versus the number of interferences for MVDR-SMI at various snapshot sizes, K.
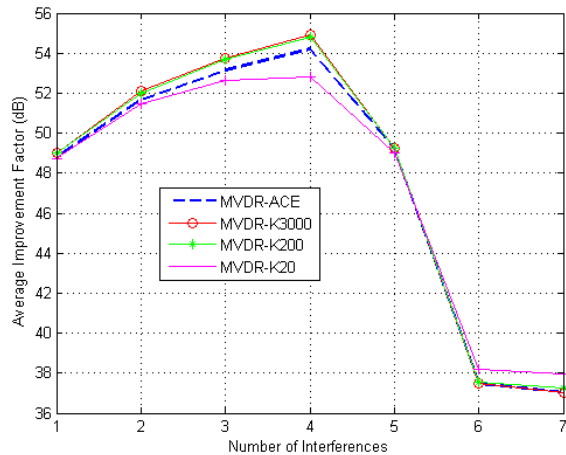
Figure 5. Scenario A: average improvement factor for MVDR-ACE, MVDR-K20, MVDR-K200 and MVDR-K3000 beamformers.


Figure 6. Scenario B: average improvement factor for MVDR-ACE, MVDR-K20, MVDR-K200 and MVDR-K3000 beamformers.

In summary, using the two multiple-interference scenarios, we have verified that a finite minimum snapshot size, such as $K \approx 2N$, can be used if the total number of interferences is less than half of the degree-of-freedoms of an N-element array. If a severe interference environment is expected, such as when the number of interference exceeds $N/2$, a significantly large snapshot size $(K > 2N)$ is recommended.

4.2. The Proposed MVDR-ACE Beamformer

Next, we analyse the performance of the MVDR-SMI beamformer employed with our proposed adaptive covariance estimator, denoted as MVDR-ACE beamformer. In the simulations, CRT is set to INR $+10 \times \log 10(N)$, which is the maximum cancellation ratio expected from an N-element array antenna [20]. From the results in Section 4.1, $L_{\max}$, is set to 3000 to align with the K value required for convergence and $L_{\min} = 20$. Δl is set to 1 for convenience of illustration. We note the choice of Δl determines the update rate of $L(t)$, and the choice will depend on the channel variation rates. As our interest in this paper is to validate the performance of the algorithm for adaptation to different number of interference signals, we chose $\Delta l = 1$. We will investigate the update rate aspect for specific channel
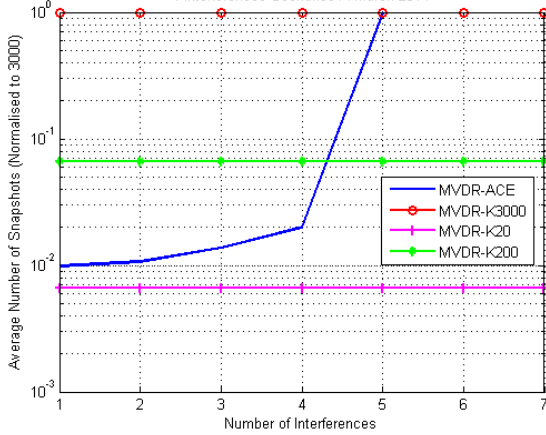
Figure 7. Scenario A: average number of snapshots for MVDR-ACE, MVDR-K3000, MVDR-K200 and MVDR-K20 beamformers.
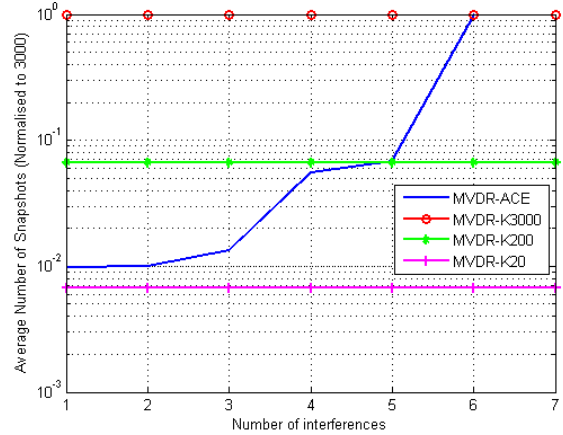
Figure 8. Scenario B: average number of snapshots for MVDR-ACE, MVDR-K3000, MVDR-K200 and MVDR-K20 beamformers.

models as our future work.

Figure 5 and Figure 6 show the average IF of the MVDR-ACE beamformer for scenarios A and B, respectively. The results for the MVDR-SMI beamformer with finite snapshot size, denoted as MVDR-K20, MVDR-K200 and MVDR-K3000 for $K = 20$, $K = 200$ and $K = 3000$ respectively, are also included for comparisons. The MVDR-K3000 result is considered as an approximation of the optimum MVDR beamformer. For different number of interferences, the results confirm that the proposed MVDR-ACE beamformer is able to maintain within a 3 dB optimum performance of the MVDR-K3000 beamformer.

The variation of the average snapshot size for scenarios A and B are shown in Figure 7 and Figure 8, respectively. The snapshot values are normalized to $K = 3000$ for clear comparison. The figures validate that the MVDR-ACE beamformer adapts its snapshot size in accordance to different interference cases. When the number of interferences is not more than $N/2$, the MVDR-ACE beamformer adapts to $\sim 1\%$ snapshot size as compared to the MVDR-K3000 beamformer, and the value is somewhere between the fixed snapshot sizes used in the MVDR-K20 and the MVDR-K200 beamformer. In severe interference cases where the number of interferences exceeds $\sim N/2$, the MVDR-ACE beamformer's snapshot size increases and approaches to the 3000 snapshots limit.

### 4.3. Instantaneous Response of MVDR-SMI & MVDR-ACE Beamformers

Section 4.2 compares the performances of MVDR-SMI and MVDR-ACE beamformers in terms of the average parameters. In this section, we compare the performance of the beamformers in terms of their instantaneous cancellation performance, $ICR_m(t)$, and include the iterative snapshot variable, $L(t)$, to illustrate the adaptive characteristic of the MVDR-ACE beamformer over multiple interferences.

For conciseness, we will present only selected interference case of scenario B. In scenario B, we recall that the MVDR-SMI beamformer in fixed snapshot size requires $K = 20$ snapshots to maintain its average SINR to be within 3 dB of the optimum performance for a maximum of 3 interferences, and it needs a higher snapshot size of $K = 200$ for the more severe interference cases. In the contrast, the MVDR-ACE beamformer maintains within the 3 dB optimum performance for all the interference cases. Therefore, we select the first severe case of four interferences and compare the performance of the beamformers using MVDR-K20, MVDR-K200 and MVDR-ACE methods. The AOAs of the four interferences are $(80°, 0°)$, $(70°, 60°)$, $(50°, 300°)$, $(60°, 0°)$. For clarity in presentation, we split the results into Figure 9, Figure 10 and Figure 11.

The top two plots of Figure 9 show the instantaneous cancellation ratio of the first interference signal, denoted as $ICR_1(t)$, that arrives at $(\theta, \phi) = (80°, 0°)$. The bottom plot of Figure 9 shows the snapshot variation of the MVDR-ACE beamformer. The figure shows that the MVDR-ACE beamformer maintains its $ICR_1(t)$ to be no less than the cancellation ratio target ($CRT = 49$ dB) by adapting its
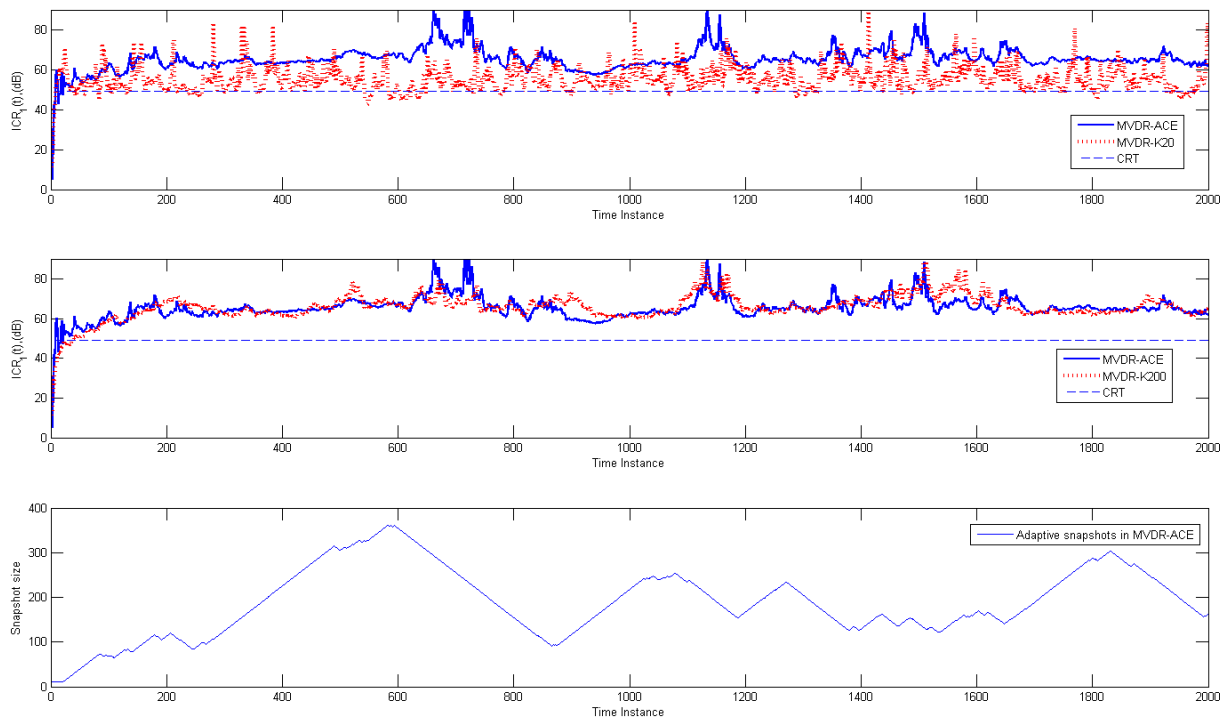
Figure 9. Scenario B, four interferences case: instantaneous cancellation ratio on interference $(80°, 0°)$ of MVDR-ACE, MVDR-K20 and MVDR-K200. The snapshot variation of the MVDR-ACE beamformer is included.
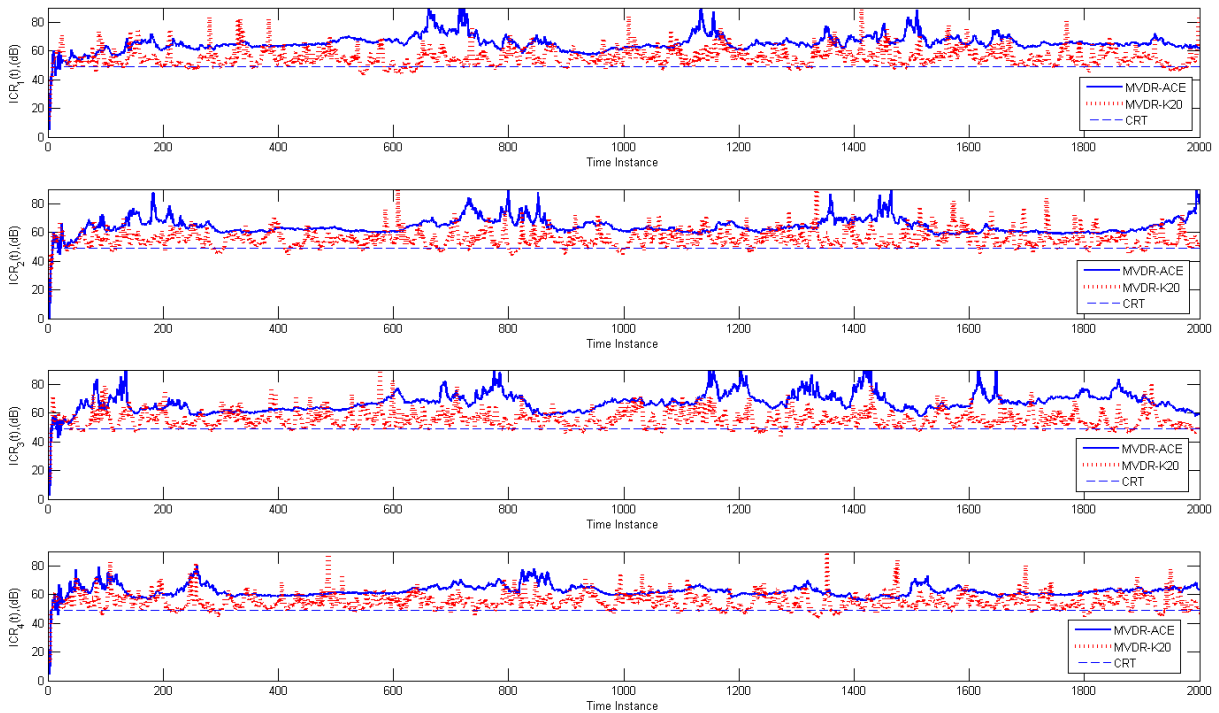
Figure 10. Scenario B, four interferences case: instantaneous cancellation ratio on all the four interferences of MVDR-ACE and MVDR-K20 beamformer.
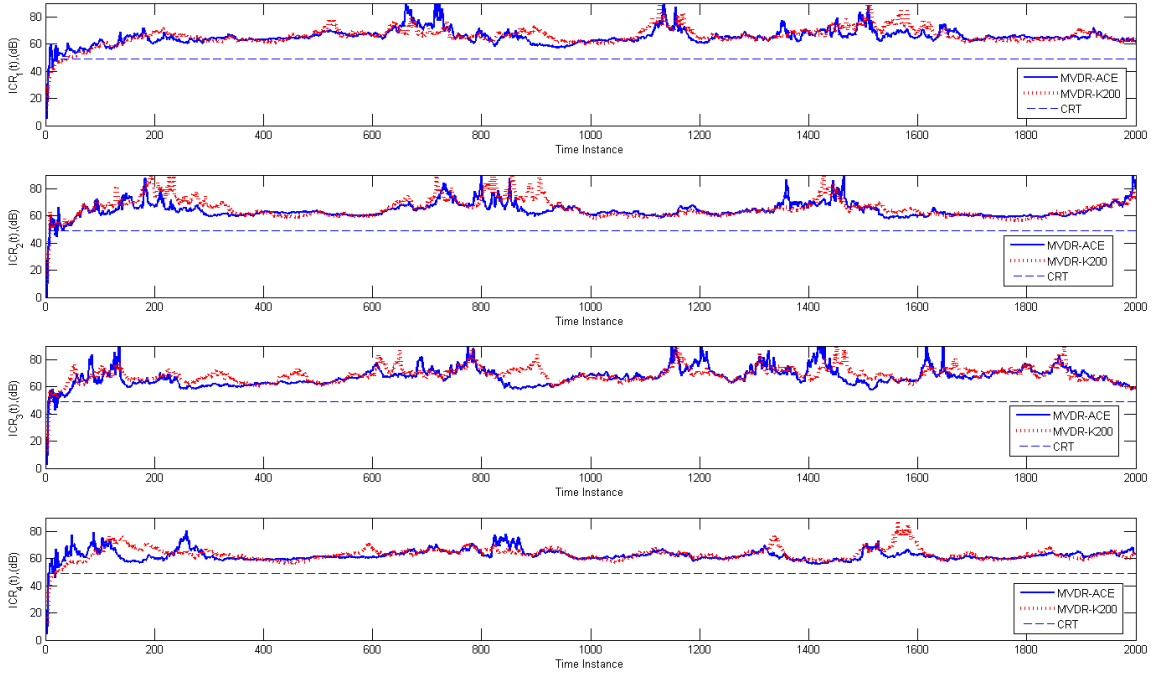
Figure 11. Scenario B, four interferences case: instantaneous cancellation ratio on interference on all the four interferences of MVDR-ACE and MVDR-K200 beamformer.

snapshot size from $L_{\min}$ at the initial time instance to values around 200 snapshots at the later time instance. The MVDR-K200 beamformer with a fixed 200 snapshots size is shown to achieve similar cancellation performance as the MVDR-ACE beamformer. In comparison, the MVDR-K20 beamformer of fixed 20 snapshot size achieves the worst interference cancellation.

Figure 10 compares the instantaneous cancellation ratio of all the interferences $(ICR_1(t) - ICR_4(t))$ for MVDR-ACE and MVDR-K20. In all cases, both beamformers achieve the same transient response up to $t = \sim 10$. This is when both beamformers use about the same snapshots size of 20. Beyond $t = \sim 10$, the MVDR-ACE beamformer always maintains better than the CRT while the MVDR-K20 beamformer obtains lower performance in several instances. The results validate that the MVDR-ACE beamformer is able to maintain within the CRT for all the interferences.

Figure 11 compares the instantaneous cancellation ratios of all the interferences for MVDR-ACE and MVDR-K200. For all interference cases, MVDR-ACE matches very well to MVDR-K200 at $t > \sim 350$. This is the time when both beamformers use about the same snapshots size of 200. The results show that the MVDR-ACE beamformer maintains the minimum number of snapshots required for the four interference cases.

5. CONCLUSIONS

Based on the MVDR-SMI method, we have proposed an adaptive MVDR-SMI beamformer using an Adaptive Covariance Estimator (ACE) to adapt to variations in the number of interference signals using minimum number of data sample size. The proposed MVDR-ACE beamformer iteratively determines a minimum number of data snapshots while maintaining its average SINR within a 3 dB performance of an optimum MVDR-SMI beamformer and also meeting a defined interference cancellation requirement.

We used Monte-Carlo simulations to validate the performance of the MVDR-ACE beamformer for an N-element uniform circular array over two sets of multiple-interference scenarios. The performances of a conventional MVDR-SMI beamformer using finite snapshot sizes are compared. Our proposed MVDR-ACE beamformer is able to iteratively determine sufficiently small data snapshots while maintaining its SINR within a 3 dB range of an optimum performance for all the interference cases.

In severe environment where the number of interferences approaches is very close to the degree-of-freedoms of the N-element array, the MVDR-ACE beamformer converges to a higher snapshot size. This is the same fixed snapshot size as would be used by the conventional MVDR-SMI beamformer to achieve its optimum performance in the severe interference environment. However, when the number of interference signals is less than $\sim N/2$, the MVDR-ACE bemformer adapts to the changes and uses about 1% to 10% snapshot size compared to the severe environment.

We will extend the study of the proposed algorithm to other applications and requirements as future works. These include applying statistical analysis to access the computational complexity of the algorithm and accessing the interference cancellation performance of other antenna geometry structures.

ACKNOWLEDGMENT

REFERENCES

1. Capon, J., "High-resolution frequency-wavenumber spectrum analysis," *Proceedings of the IEEE*, Vol. 57, No. 8, 1408–1418, 1969.
2. Haykin, S., *Adaptive Filter Theory*, 4th Edition, Prentice Hall, New Jersey, 2002.
3. Carlson, B. D., "Covariance matrix estimation errors and diagonal loading in adaptive arrays," *IEEE Trans. Aerospace and Electronic Systems*, Vol. 24, No. 4, 397–401, Jul. 1988.
4. Elnashar, A., S. M. Elnoubi, and H. A. El-Mikati, "Further study on robust adaptive beamforming with optimum diagonal loading," *IEEE Trans. Antennas Propagat.*, Vol. 54, No. 12, 3647–3658, Dec. 2006.
5. Besson, O. and F. Vincent, "Performance analysis of beamformers using generalized loading of the covariance matrix in the presence of random steering vector errors," *IEEE Trans. Signal Process.*, Vol. 53, No. 2, 452–459, Feb. 2005.
6. Stocia, P., Z. Wang, and J. Li, "Robust capon beamforming," *IEEE Signal Processing Letters*, Vol. 10, No. 6, 172–175, May 2003.
7. Vorobyov, S. A., A. B. Gershman, and Z. Q. Luo, "Robust adaptive beamforming using worst-case performance optimization," *IEEE Signal Processing Letters*, Vol. 51, 313–324, Feb. 2003.
8. Liu, F., J. Wang, C. Y. Sun, and R. Du, "Robust MVDR beamformer for nulling level control via multi-parametric quadratic programming," *Progress In Electromagnetics Research C*, Vol. 20, 239–254, 2011.
9. De Natale, F., M. Donelli, S. Caorsi, D. Franceschini, and A. Massa, "A versatile enhanced genetic algorithm for planar array design," *Journal of Electromagnetic Wave and Applications*, Vol. 18, No. 11, 1533–1548, 2004.
10. Massa, A., F. de Natale, S. Caorsi, M. Donelli, and A. Lommi, "Planar array control with genetic algorithms and adaptive array theory," *IEEE Trans. Antenna Propagat.*, Vol. 52, No. 11, 2919–2924, 2004.
11. Widrow, B., K. Duvall, R. Gooch, and W. Newman, "Signal cancellation phenomena in adaptive antennas: Causes and cures," *IEEE Trans. Antennas Propagat.*, Vol. 30, No. 3, 469–478, May 1982.
12. Boroson, D. M., "Sample size considerations for adaptive arrays," *IEEE Trans. Aerospace and Electronic Systems*, Vol. 16, No. 4, 446–451, Jul. 1980.
13. Grantz, M. W., R. L. Moses, and S. L. Wilson, "Convergence of the SMI and the diagonally loaded SMI algorithms with weak interference," *IEEE Trans. Antennas Propagat.*, Vol. 38, No. 3, 394–399, Mar. 1990.
14. Brookner, E. and J. M. Howell, "Adaptive-adaptive array processing," *Proceedings of the Phased Arrays Symposium*, 133, 1985.
15. Reed, I. S., J. D. Mallett, and L. E. Brenna, "Rapid convergence rate in adaptive arrays," *IEEE Trans. Aerospace and Electronic Systems*, Vol. 10, No. 6, 853–863, Nov. 1974.

16. Hara, Y., "Weight-convergence analysis of adaptive antenna arrays based on SMI algorithm," *IEEE Trans. Wireless Communications*, Vol. 2, No. 4, 749–757, Jul. 2003.

17. Zhang, L., W. Liu, and L. Yu, "Performance analysis for finite sample MVDR beamformer with forward backward processing," *IEEE Trans. Signal Process.*, Vol. 59, No. 5, 2427–2431, May 2011.

18. Pados, D. A. and G. N. Karystinos, "An iterative algorithm for the computation of the MVDR filter," *IEEE Trans. Signal Process.*, Vol. 49, No. 2, 290–300, Feb. 2001.

19. Hudson, J. E., *Adaptive Array Principles*, Peter Peregrinus Ltd.-IET, 1981.

20. Farina, A., *Antenna-based Signal Processing Techniques for Radar Systems*, Artech House, Inc., Norwood, MA, 1992.

21. Baseri, R., K. B. Yu, and M. A. Hussain, "Testing adaptive jamming cancellation algorithms using a digital beamforming array," *Proc. IEEE Nat. Radar Conf.*, 314–319, Syracuse, NY, May 1997.

22. Compton, R. T., *Adaptive Antennas: Concepts and Performance,* Prentice Hall, New Jersey, 1988.

23. Horowitz, L. L., H. Blatt, W. G. Brodsky, and D. K. Senne, "Controlling adaptive arrays with the sample matrix inversion algorithm," *IEEE Trans. Aerospace and Electronic Systems*, Vol. 15, No. 6, 840–847, Nov. 1979.

24. Widrow B. and J. M. McCool, "A comparison of adaptive algorithms based on the methods of steepest descent and random search," *IEEE Trans. Antennas Propagat.*, Vol. 24, No. 5, 615–637, Sep. 1976.

25. Loecker, C., P. Knott, R. Sekora, and S. Algermissen, "Antenna design for a conformal antenna array demonstrator," *2012 6th European Conference on Antennas and Propagation (EUCAP)*, 151–153, 2012.

26. Kasemodel, J. A., C.-C. Chen, I. J. Gupta, and J. L. Volakis, "Miniature continuous coverage antenna array for GNSS receivers," *IEEE Antennas And Wireless Propagation Letters*, Vol. 7, 592–595, Dec. 2008.